Separation and Purification Technology 378 (2025) 134691

Contents lists available at ScienceDirect

Separation and Purification Technology

journal homepage: www.elsevier.com/locate/seppur

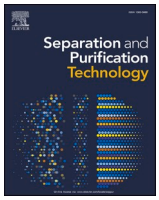

Data-driven prediction of copper leaching yield from brass waste using stacking ensemble learning

Sercan Basit [a,*], Murat Uyar [b]

[a] Kırşehir Ahi Evran University, Department of Mechanical Engineering, Kırşehir 40100, Türkiye
[b] Bursa Uludag University, Department of Electrical-Electronics Engineering, Bursa 16059, Türkiye

ARTICLE INFO

Editor: Rajiv R. Srivastava

Keywords:
Brass waste
Copper leaching
Stacking ensemble learning
Hydrometallurgical recovery
Machine learning prediction

ABSTRACT

The recovery of valuable metals from industrial waste has become increasingly important due to the diminishing supply of primary resources and growing environmental concerns. This paper presents a stacking ensemble learning method for predicting copper leaching yield from brass melting slag under different hydrometallurgical conditions. Instead of conducting time-consuming and complex experiments, a machine-learning approach was built using a large dataset previously collected through controlled laboratory research. Six experimental variables were used as input features, including leaching time, acid concentration, hydrogen peroxide concentration, stirring speed, temperature, and solid-to-liquid ratio. The proposed model combines three tuned base learners, namely Gaussian process regression, least-squares boosting, and support vector regression, with a linear regression meta-learner. The stacking model achieved all individual models in predictive performance, yielding the lowest RMSE of 0.853, MAE of 0.668, and MAPE of 8.347 %, resulting in the highest R^2 value of 0.994. The results demonstrate that the proposed method is reliable and practically feasible for predicting leaching yield and optimizing the recovery process of copper from brass waste. Furthermore, it has significant potential for supporting resource management objectives.

1. Introduction

The recovery of precious metals from industrial waste is significant for countries with scarce natural resources. Such efforts directly contribute to environmental protection and resource conservation goals [1]. In recent years, as technology advances and industrial production expands, the demand for critical and precious metals has increased significantly [2]. However, the decrease in primary mineral reserves and the damage caused to the environment by traditional mining methods have brought the importance of recovering metals from secondary sources to prominence. This situation has made recovering valuable metals from industrial waste an essential and sustainable alternative. In particular, the effective use of metallurgical waste contributes to the efficient use of resources and environmental sustainability. It is also consistent with the goals of the green economy, which promotes economic circularity [3].

Brass is an alloy mainly composed of the elements copper and zinc. It is widely used in industries such as construction, electronics, automotive, and healthcare due to its mechanical strength, corrosion resistance, antimicrobial properties, and electrical conductivity [4,5]. Its relatively low production cost and high workability make brass an economical and viable option for various applications [6]. According to current market forecasts, the global brass industry, which was valued at approximately US$22.5 billion in 2024, is expected to exceed US$30 billion by 2032. This growth corresponds to a compound annual growth rate of roughly 3.8 % for 2023–2032 [7]. However, this growing demand is leading to a significant increase in the generation of brass-related waste during the production and post-consumption stages. At the same time, the decreasing availability and rising cost of primary sources of base metals such as copper and zinc make brass waste a valuable secondary resource for metal recovery. Previous research has shown that brass waste can contain up to 50 % zinc and approximately 20 % copper, making recovery of these wastes economically attractive [8]. Accordingly, managing and recycling these wastes is essential to reduce environmental burdens and support consistent access to raw materials in industrial operations [9–11].

The recovery of copper and zinc from brass waste is usually performed through pyrometallurgical or hydrometallurgical methods [12]. While pyrometallurgical approaches require high energy consumption and may lead to atmospheric gas emissions, hydrometallurgical

* Corresponding author.
E-mail address: sercan.basit@ahievran.edu.tr (S. Basit).

https://doi.org/10.1016/j.seppur.2025.134691
Received 3 April 2025; Received in revised form 24 July 2025; Accepted 7 August 2025
Available online 8 August 2025

techniques offer several advantages, such as lower processing temperatures, selective metal dissolution, and better suitability for small-scale operations [8,12,13]. Specifically, sulfuric acid-based leaching procedures, sometimes combined with oxidizing agents such as hydrogen peroxide, have demonstrated high extraction efficiencies for zinc and copper under optimized conditions. Recent efforts have focused on optimizing alternative leaching systems customized according to recovery process conditions. For example, Maleki et al. [12] applied a pyro-hydrometallurgical method involving high-temperature oxidation at 850–900 °C followed by sulfuric acid leaching. The thermal pretreatment altered the phase composition of the slag, significantly improving metal solubility. As a result, a total recovery efficiency of 81 % was achieved for zinc and copper combined. Martins et al. [8] investigated the recovery of zinc and copper from brass waste through a hydrometallurgical process incorporating sulfuric acid leaching and solvent extraction using D2EHPA. Zinc extraction reached 91.9 % when leaching was conducted at pH 2, 80 °C, and a sulfuric acid concentration of 0.8 M. In the subsequent stripping phase using an industrial solution (~1.8 M H_2SO_4), zinc recovery increased to 96.9 %, while copper dissolution remained relatively low at 42.2 %. These results confirm that sulfate-based systems can achieve high zinc recovery rates, whereas copper recovery remains sensitive to leaching conditions and media composition. Therefore, the choice of leaching medium should be aligned with specific recovery priorities and process constraints. Similarly, Xia et al. [13] developed a $ZnCl_2$–NH_4Cl-based leaching process to extract zinc and copper from brass smelting slag. At 95 °C, the learning efficiencies of approximately 88.4 % for zinc and 90.9 % for copper were achieved. These results demonstrate the effectiveness of the chloride–ammonia system as a selective and efficient medium for metal recovery from complex secondary resources. Huang et al. [14] developed a selective complexation method using an alkaline glycine solution to recover copper from smelting slag. They optimized parameters such as pH, particle size, temperature, liquid-to-solid (L/S) ratio, and glycine concentration to achieve copper selectivity. At pH 10 and 40 °C with 100 g/L glycine, a copper leaching efficiency of 86.40 % was achieved, while other metals such as iron, lead, and zinc remained mostly undissolved. Glycine forms stable complexes with copper, enabling selective leaching. Kinetic analyses revealed that the leaching process followed a mixed control mechanism, governed by internal diffusion and interfacial chemical reactions. Despite these advancements, hydrometallurgical methods often require careful optimization due to drawbacks, such as high reagent consumption, effluent treatment needs, and corrosion risks [12].

Optimizing leaching parameters is essential for effective hydrometallurgical processes. Key parameters include acid concentration, temperature, leaching time, oxidant dosage, and solid-to-liquid (S/L) ratio [15]. Proper optimization maximizes recovery efficiency and minimizes chemical consumption and environmental impact [16,17]. Traditional methods, such as single-variable optimization and response surface methodology, have been employed to investigate the influence of individual parameters on metal leaching efficiency [18]. However, such approaches often fail to capture nonlinear interactions in multi-parameter systems, where process behavior tends to be highly interdependent [17,19]. Additionally, traditional methods often rely on trial-and-error experimentation, which can be time-consuming, resource-intensive. As a result, there is growing interest in computational tools that enable data-driven optimization of these processes. To overcome the limitations of traditional methods, machine learning (ML) and artificial intelligence (AI) techniques have recently emerged as powerful alternatives for modeling complex chemical systems, including metal leaching [20–23]. These techniques can learn hidden patterns from existing experimental data. They generate predictive models that facilitate accurate forecasting, sensitivity analysis, and decision-making support without exhaustive experimentation. Consequently, integrating ML into hydrometallurgical research enables quantitative optimization of multiple parameters simultaneously, reducing experimental overhead while improving process efficiency and resource utilization in metal recovery operations.

Several recent studies have applied ML approaches to predict metal leaching efficiency under various experimental conditions [23–26]. Ordaz-Oliver et al. [27] conducted a laboratory-scale study on copper recovery from printed circuit boards using dynamic acid leaching. They developed an artificial neural network (ANN) model to predict copper dissolution based on varying stirring ratios. The study revealed that the ANN model exhibited an outstanding prediction performance, achieving a coefficient of determination (R^2) of 0.9969, a mean square error (MSE) of 0.0286, and a mean absolute error (MAE) of 0.1341. Zhang et al. [17] applied ML techniques to assess the influence of multiple leaching parameters. Their findings revealed that the most influential variables were the leaching time, sulfuric acid concentration, and ferrous sulfate concentration. Among the models tested, support vector regression (SVR) outperformed others ($R^2 = 0.92$, MSE = 25.04), highlighting its suitability for hydrometallurgical optimization. Similarly, Sobouti et al. [16] employed ML approaches to predict metal recovery from lead concentrate. Their ANN-PSO model utilized input features such as leaching time, liquid-to-solid ratio, stirring speed, temperature, and acid concentration. With reported accuracies of $R^2 = 0.99$ for training and $R^2 = 0.95$ for testing, the model was found to be effective for optimization without requiring extensive experimental trials. Despite promising results, many studies in the literature are based on small datasets [16,23,28], which raises concerns about model overfitting and generalizability. Furthermore, some evaluations have considered only a limited number of leaching parameters [27,29], restricting the scope of analysis. To improve the accuracy of optimization and yield prediction models, a more comprehensive evaluation of key leaching parameters, such as time, acid concentration, stirring speed, temperature, solid–liquid ratio, and pH, is required [16,17,30].

These models, often developed using limited datasets, have successfully predicted leach yield based on input parameters such as leaching time, acid concentration, temperature, stirring speed, and oxidant dosage. However, several studies fall short in providing sufficient justification for the selection of ML algorithms or lack a systematic comparison of alternative models within a unified framework. Most importantly, to our knowledge, no existing research has yet employed a stacked ensemble learning approach to predict copper leaching yield from brass waste. This reveals a significant gap in the literature and underscores the need for robust, multi-model architectures capable of capturing the complex, nonlinear, and interactive dynamics inherent in the leaching process.

This study proposes a novel stacking ensemble learning approach to predict the copper leaching yield from brass melting slag under varying process conditions. Instead of conducting new long-term and prior experiments, this research leverages an extensive experimental dataset previously obtained through systematic laboratory trials. Six key input parameters were used to model the leaching process, namely leaching time, acid concentration, hydrogen peroxide concentration, stirring speed, temperature, and S/L ratio. The proposed approach combines the predictive capabilities of three optimized base learners, namely Gaussian process regression (GPR), least-squares boosting (LSBoost), and SVR, with a linear regression (LR) meta-learner to capture complex nonlinear interactions. The performance of the stacking model was evaluated and compared against individual models using multiple statistical metrics and cross-validation to ensure robustness. This study provides an interpretable tool for yield prediction and offers a cost-effective and scalable strategy for optimizing hydrometallurgical recovery processes from brass waste.

The main innovative contributions of this study can be given as follows:

- A stacked ensemble learning model was developed by integrating GPR, SVR, and LSBoost base learners with a linear meta-learner to

predict copper leaching yield with improved accuracy and generalization.

- This is the first study to apply ML to copper recovery from brass melting slag, addressing a gap in the literature on secondary industrial waste sources.
- The study demonstrated a data-driven strategy for improving hydrometallurgical process efficiency and scalability without requiring additional long-term experiments.
- A dataset comprising 219 systematic leaching experiments was used, offering greater sample diversity than most previous studies and improving model reliability under varying process conditions.

2. Materials and methods

This section presents the materials utilized in the study, the experimental procedures applied, and the modeling approaches developed. The initial stages of the research involved material preparation,

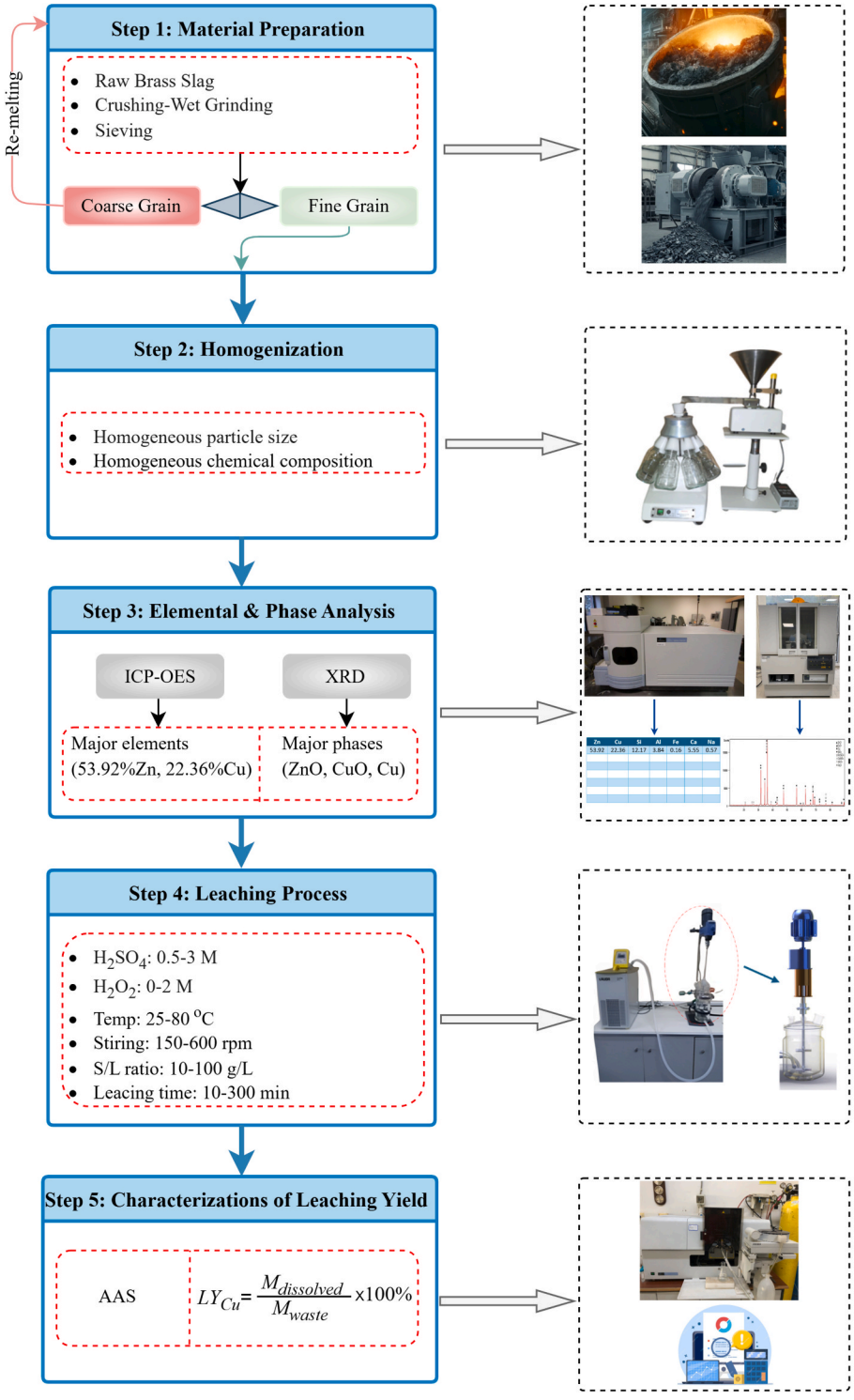

Fig. 1. Flowchart of the experimental study.

homogenization, and elemental and phase analyses, which were carried out to ensure uniformity and accurate characterization of the raw brass slag. Subsequently, leaching experiments were performed using sulfuric acid under varying process conditions, and detailed information regarding this stage is provided. A dataset comprising leaching input parameters and their corresponding yield outcomes was constructed based on the experimental results. Finally, the theoretical foundations, structural configurations, and parameter settings of the ML algorithms employed for modeling and predicting copper leaching yield are comprehensively described.

2.1. Experimental setup and workflow

The experimental design followed a structured series of hydrometallurgical procedures under controlled laboratory conditions. As illustrated in Fig. 1, the workflow encompassed five essential stages: (i) collection of brass melting slag as the raw material, (ii) particle size reduction and mechanical homogenization, (iii) chemical and mineralogical characterization, (iv) leaching experiments under varying process conditions, (v) quantification of copper yield. Each of these stages is detailed in the subsequent subsections. A complete list of instruments used throughout the experimental study, along with their manufacturers and model numbers, is summarized in Table S1 of the Supplementary Material.

2.1.1. Material preparation and homogenization

The brass waste used in this study was supplied by Özer Metal A.Ş., located in Çerkezköy, Istanbul. The raw material, composed of brass-melting slags, first underwent a series of preparatory steps, including crushing, wet grinding, and sieving. These processes were employed to reduce the particle size and to obtain more uniform material fractions suitable for subsequent analyses and leaching procedures. Following the sieving stage, the material was classified into coarse and fine grain categories based on particle size distribution.

To ensure the consistency and reproducibility of the experimental results, the fine fractions were subjected to mechanical homogenization using a dedicated homogenization device, as illustrated in Fig. 1. This process was designed to achieve uniformity in particle size distribution and chemical composition across all experimental batches. Grain size measurements were conducted using a Malvern 2000 Mastersizer, which indicated an average particle size of 193.851 μm. A complementary sieve analysis was performed to validate the accuracy of these results. The close agreement between the two methods confirmed the reliability of the particle size data. This combined preparation and homogenization procedure was essential for minimizing variability in the raw material, thereby enhancing the reliability of the leaching experiments in subsequent phases.

2.1.2. Elemental and phase characterization

After homogenization, representative subsamples were collected to perform chemical and mineralogical analyses. The chemical composition of the homogenized brass waste was determined using inductively coupled plasma optical emission spectroscopy (ICP-OES). As presented in Table 1, the material was found to contain a substantial amount of copper, comprising 22.36 % by weight, representing this study's primary target element. In addition to copper, the brass waste includes 53.92 % zinc, 12.17 % silicon, and 3.84 % aluminum. Smaller quantities of calcium, sodium, and iron were also identified, with concentrations of 5.55 %, 0.57 %, and 0.16 %, respectively. The elevated levels of copper and zinc suggest that waste is a promising candidate for hydrometallurgical recovery processes.

Table 1
Chemical composition of the homogenized brass waste (wt%).

Zn	Cu	Si	Al	Fe	Ca	Na
53.92	22.36	12.17	3.84	0.16	5.55	0.57

Note: Only major components are reported.

Mineralogical analysis was carried out using X-ray diffraction (XRD) to assess further the structural factors influencing copper leachability. The XRD pattern, presented in Fig. 2, confirmed the presence of crystalline copper-bearing phases such as CuO and Cu, which have direct implications for the leaching behavior of the material. Several other phases were identified, including ZnO, SiO_2, Al_2O_3, Fe_2SiO_4, $CaSO_4$, and FeO. Although these non-copper phases are not the focus of the present study, they may influence the leaching kinetics and selectivity due to their interaction within the multiphase matrix.

The waste material was comprehensively characterized using ICP-OES and XRD, particularly copper-bearing constituents. The combination of preliminary homogenization and detailed characterization ensured consistency across experimental batches. It enabled a focused evaluation of copper recovery behavior, forming a robust foundation for the ML-based predictive modeling developed in this study.

2.1.3. Leaching experiments and yield determination

The leaching experiments were designed to evaluate the influence of fundamental process parameters on copper recovery efficiency over time. The parameters studied included the concentration of sulfuric acid (H_2SO_4: 0.5, 1, 2, and 3 M), hydrogen peroxide (H_2O_2: 0, 0.5, 0.75, 1, 1.5, and 2 M), reaction temperature (25, 40, 60, and 80 °C), stirring speed (150, 300, 450, and 600 rpm), and S/L ratio (10, 20, 50, and 100 g/L). All experiments were performed in a 1-liter, temperature-controlled glass reactor equipped with a mechanical stirrer and an in-line pH probe to maintain stable operating conditions. Each leaching trial was conducted for 300 min, during which solution samples were collected at predetermined time intervals: 10, 20, 30, 40, 60, 120, 180, 240, and 300 min. The collected samples were immediately filtered using standard filter paper and diluted as required before analysis. Copper concentrations in the filtrates were determined using a Perkin Elmer flame atomic absorption spectrometer (AAS). The selection of experimental parameters was based on two primary considerations:

- The parameter ranges reported in previous studies on the hydrometallurgical leaching of brass slag [9,31]
- The necessity to explore both low and high-end conditions to ensure model generalizability and process insight.

These selected parameter ranges ensured that the experimental framework covered a representative spectrum of both laboratory- and industry-scale leaching conditions, while also allowing the resulting dataset to capture potential nonlinear behaviors across a broad operational domain.

The copper leaching yield was calculated using Eq. (1):

$$LY_{Cu} = \left(\frac{M_{dissolved}}{M_{waste}}\right) \times 100\% \quad (1)$$

where LY_{Cu} represents the copper leaching yield (%), $M_{dissolved}$ is the amount of dissolved copper in the solution (g), and M_{waste} denotes the total copper content in the brass waste before leaching (g).

To develop a robust and data-rich modeling framework, 219 leaching experiments were systematically conducted to investigate the combined effects of key process parameters on copper recovery efficiency. In this extensive and time-consuming experimental effort, a comprehensive dataset covering a wide range of operating conditions was generated. The resulting data were subsequently utilized to develop ML models to predict leaching efficiency and optimize process performance.

2.2. Machine learning models for leaching yield prediction

Various ML models were evaluated to predict copper leaching yield based on experimental parameters. Each model had distinct strengths in

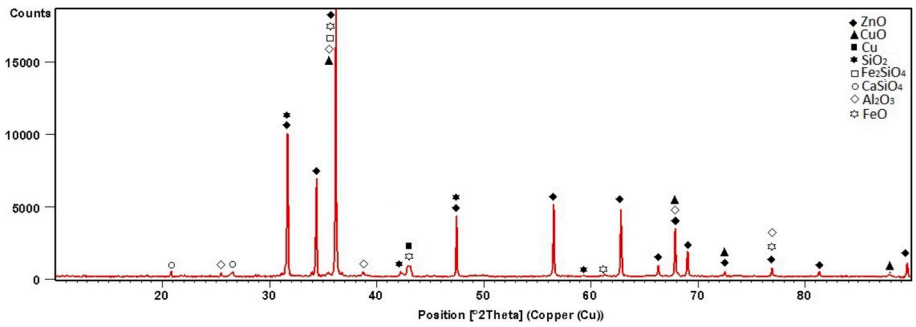

Fig. 2. XRD analysis results of waste materials.

capturing complex relationships and ensuring reliable generalization. The selected models include GPR, SVR, random forest (RF), LSBoost, and multi-layer perceptron (MLP). The selection of these models was driven by their capability to capture nonlinear relationships, generalize well across different data distributions, and balance interpretability with computational efficiency. The mathematical formulations, hyperparameters, and reasons for selecting each model are detailed below.

2.2.1. Dataset description

The dataset used in this study consists of multiple independent variables, representing the key experimental parameters that influence the leaching process, along with a single dependent variable, which quantifies the copper leaching yield. The independent variables were carefully selected to reflect the main operational conditions affecting metal dissolution. These parameters include the stirring speed (rpm), which regulates the mass transfer rate and reaction kinetics; the H_2O_2 concentration (M), which serves as an oxidizing agent to enhance metal dissolution; the temperature (°C), which affects reaction rates and solubility; the S/L ratio (g/L), representing the mass fraction of solid material in the solution; the leaching time (min), which determines the reaction time for metal dissolution; and the acid molarity (M), which regulates the acidity of the leaching solution and directly influences dissolution efficiency. The dependent variable is the copper leaching yield, representing the proportion of copper extracted from the waste material relative to its initial content. This value serves as the primary performance metric for evaluating the effectiveness of the leaching process.

Since the input features in the dataset exhibit varying scales, min–max scaling normalization was applied as a preprocessing step. This technique transforms each feature into a fixed range, typically [0, 1], ensuring that no single variable dominates the learning process due to its magnitude. The min–max scaling formula is expressed in Eq. (2):

$$X_{norm} = \frac{X - X_{min}}{X_{max} - X_{min}} \tag{2}$$

where X is the original feature value, X_{min} and X_{max} are the minimum and maximum values of the feature, and X_{norm} is the resulting normalized value. This normalization strategy retains the relative distribution of data points while reducing the influence of varying feature magnitudes, permitting successful and balanced model training [32].

k-fold cross-validation was used to increase the prediction models' generalization performance. This approach divides the dataset into k subsets of equal size (folds). For each iteration, the model is trained using k–1 folds and validated on the remaining fold. This process is repeated k times, allowing each fold to be the validation set once. The final performance of the model is then computed as the average of all iterations, ensuring a more robust and unbiased evaluation [33].

2.2.2. Gaussian process regression

GPR is a non-parametric Bayesian approach to regression that provides probabilistic predictions, making it particularly advantageous for modeling complex, nonlinear relationships in small datasets [34]. Unlike parametric models, which assume a fixed functional form, GPR models are distributed over all possible functions that could explain the observed data, thereby offering both a mean prediction and an uncertainty estimate [35].

A Gaussian process is defined as a collection of random variables, any finite subset of which follows a multivariate normal distribution. Given a training dataset $\{(X_i, y_i)\}_{i=1}^{n}$, where X_i represents the input feature vector, and y_i is the corresponding target value, GPR assumes that the function $y(X)$ follows a Gaussian process:

$$y(X) \ \mathcal{GP}(m(X), K(X, X')) \tag{3}$$

where $m(X)$ represents the mean function, and $K(X, X')$ is the covariance kernel function, which defines the similarity between data points. The primary hyperparameters that require optimization in this method include the choice of kernel function (radial basis function (RBF), Matern, or rational quadratic), the length scale parameter, and the noise variance [34].

In this study, the Matern 3/2 kernel function was selected due to its suitability for modeling moderately smooth relationships between the input features and copper leaching yield. The kernel scale parameter, which determines the spatial sensitivity of the kernel function, was optimized and set to 0.7613. The noise standard deviation (σ), which reflects the assumed measurement uncertainty in the data, was set to 1.1113 to effectively control model flexibility and avoid overfitting. All input features were standardized before modeling to ensure numerical stability and improve the convergence of the training process. The optimization of the GPR model's hyperparameters was conducted using a Bayesian optimization strategy, which systematically explores the hyperparameter space by building a surrogate model and selecting new candidates based on acquisition functions [36]. This approach enables efficient and intelligent parameter tuning, especially in cases where model evaluations are computationally expensive or the search space is complex [37]. Model performance was evaluated using a 10-fold cross-validation scheme, which provides robust and generalizable estimates of predictive accuracy across different data splits. The same Bayesian optimization and validation procedure was consistently applied to all other ML models in this study, ensuring a standardized and fair comparison of model performance.

2.2.3. Support vector regression

SVR is a powerful supervised learning algorithm based on support vector machines (SVMs), designed to perform regression tasks by mapping input data into a high-dimensional feature space using kernel functions [36]. SVR introduces a margin of tolerance (∈) around the true values, enabling prediction flexibility while maintaining robustness against overfitting, distinguishing it from methods that focus solely on minimizing squared error [38].

Given a training dataset $\{(X_i, y_i)\}_{i=1}^{n}$, where X_i represents the input feature vector, and y_i is the corresponding target value, SVR aims to find

a function $f(X)$ that approximates the relationship between inputs and outputs while maintaining a margin of tolerance ∈. The general form of the SVR model is expressed in Eq. (4).

$$y(X) = \omega^T \phi(X) + b \tag{4}$$

where $y(X)$ denotes the predicted output of the SVR model for the input vector X, $\phi(X)$ represents the transformation to a higher-dimensional space, ω is the weight vector, and b is the bias term. To achieve optimal performance, SVR hyperparameters need to be fine-tuned, including the kernel type (linear, polynomial, or Gaussian RBF), the regularization parameter (C), the margin tolerance (∈), and the kernel coefficient (γ) [39].

In this study, a Gaussian RBF kernel function was selected to effectively capture nonlinear relationships between input features and leaching yield. The kernel scale parameter was optimized and set to 0.52, determining the range over which a single training example influences predictions, as it is inversely related to the gamma parameter in the RBF kernel. The box constraint parameter (C), which controls the trade-off between achieving a low error and avoiding overfitting, was optimized at 132. The epsilon (∈) parameter, which defines the margin of tolerance for errors in the SVR model, was fine-tuned to 0.014579.

2.2.4. Random forest

RF is a powerful ensemble learning algorithm that constructs multiple decision trees (DTs) and aggregates their predictions to improve accuracy, stability, and generalizability [40]. Unlike a single decision tree, which is prone to overfitting and high variance, RF mitigates these issues by introducing randomness in both the data sampling process and the selection of features [41].

X, a p-dimensional input vector, is used to construct the DTs in the RF model. A set of T trees, denoted as $\{h_1(x), h_2(x),\ldots, h_T(x)\}$, is trained independently using bootstrapped subsets of the data, introducing variability and reducing overfitting [41]. The final prediction of the RF model is obtained by averaging the outputs of all trees, as expressed in the following equation:

$$y(X) = \frac{1}{T}\sum_{t=1}^{T} h_t(X) \tag{5}$$

where $y(X)$ represents the final prediction of the model for the input vector X, $h_t(X)$ denotes the prediction from each decision tree, and T is the number of trees in the ensemble. The key hyperparameters to be optimized in this method are the number of trees, maximum depth, and minimum samples per split [41].

In this study, the number of trees was set to 60, ensuring a balance between model complexity and computational efficiency. The maximum number of splits was determined to be 34, controlling the depth of each DT to prevent overfitting while maintaining sufficient flexibility in decision boundaries. Additionally, the minimum leaf size was optimized at 1, regulating the minimum number of samples required to create a leaf node. The model was trained using the bagging method, leveraging bootstrapped datasets to enhance stability.

2.2.5. Least-squares boosting

LSBoost is a gradient boosting algorithm that creates a very effective predictive model by sequentially combining weak learners [42]. Unlike other ensemble approaches that train a series of individual models and aggregate their predictions separately, LSBoost refines predictions incrementally by shrinking residual errors of previous steps [43]. This makes LSBoost very effective at extracting complex patterns in data and avoiding bias without compromising model flexibility [42].

The LSBoost algorithm follows an iterative learning process in which a weak learner $h_m(X)$ is added at each iteration to improve the overall model prediction. The updated model at iteration m is expressed as:

$$F_m(X) = F_{m-1}(X) + \lambda h_m(X) \tag{6}$$

where $h_m(X)$ is the weak learner at iteration m, λ is the learning rate, and $F_m(X)$ represents the updated model. The key hyperparameters to be optimized in this method are the learning rate, number of estimators, maximum number of splits, and minimum leaf size [42].

In this study, the number of estimators was set to 122, balancing computational cost and predictive performance. The learning rate was optimized at 0.1, determining the step size at each iteration to refine the weak learners. The maximum number of splits was set to 14, controlling the complexity of individual decision trees to prevent overfitting. Additionally, the minimum leaf size was optimized at 1, ensuring sufficient samples per leaf node for stable learning.

2.2.6. Multi-layer perceptron

MLP is a type of ANN designed to learn complex patterns by applying a series of linear transformations followed by nonlinear activation functions [44]. It is particularly effective in capturing nonlinear dependencies in datasets, making it well-suited for leaching yield prediction.

Mathematically, the transformation performed by a multi-layer MLP model can be expressed as:

$$y(X) = W^L \bullet h^{(L-1)} + b^L \tag{7}$$

where each hidden layer output is computed recursively as:

$$h^{(l)} = \sigma^{(l)}\left(W^{(l)} \bullet h^{(l-1)} + b^{(l)}\right), l = 1, 2, \cdots, L-1$$

and initial input:

$$h^{(0)} = X$$

X denotes the input feature vector, $y(X)$ represents the predicted output, $W^{(l)}$ and $b^{(l)}$ refer to the weight matrix and bias vector at the l^{th} layer, respectively, $\sigma^{(l)}(\cdot)$ is the nonlinear activation function applied at the l^{th} layer, $h^{(l)}$ denotes the output of the l^{th} hidden layer, and L is the total number of layers, including the final output layer. Several hyperparameters must be optimized to enhance MLP's predictive performance, including the number of hidden layers and neurons, the activation function, the learning rate, and the optimizer [44,45].

In this study, the network architecture consisted of two hidden layers, with 6 and 22 neurons forming an optimized structure for capturing complex data relationships. The activation function was set to logsig in the hidden layers, as it is well-suited for capturing nonlinear dependencies that are characteristic of leaching behavior. Meanwhile, a purelin activation function was used in the output layer to allow for unbounded linear mapping, which is appropriate for continuous-valued yield prediction. The Levenberg-Marquardt (trainlm) learning algorithm was employed to enhance optimization efficiency.

Previous studies indicate that GPR is particularly effective for small datasets with complex nonlinearities, while SVR performs well in high-dimensional feature spaces with appropriate kernel selection. RF is advantageous in handling noisy datasets and reducing variance, whereas LSBoost enhances predictive accuracy by iteratively refining weak learners. Finally, MLP excels in capturing hierarchical relationships in data but requires careful hyperparameter tuning to avoid local minima. Their comparative performance is systematically evaluated in Section 4.

2.2.7. Stacking ensemble model

Stacking ensemble learning is a well-established paradigm in ML that combines the strengths of multiple base learners to improve predictive performance and generalization [46,47]. The key idea behind stacking is the use of a two-level learning framework: first, multiple base models are trained on the original dataset, and then a secondary model, called the meta-learner, is trained on the predictions made by the base models [48,49]. This strategy enables the model to capture nonlinear patterns and interactions that might be missed by individual models [50].

The main advantage of stacking lies in its ability to reduce generalization error and mitigate overfitting by leveraging the diversity and complementary nature of different learning algorithms [50]. As stated by ref. [49], stacking ensemble methods improves prediction accuracy and stability by learning how to best combine the outputs of diverse base learners. These learners may vary in structure, learning capacity, or underlying assumptions and thus offer different perspectives on the same problem. The meta-learner integrates these insights, often through a simple linear or nonlinear combination, resulting in improved forecasting capabilities [51].

Mathematically, the stacking model can be formulated as follows:

Let the training data be denoted as

$$\mathscr{D} = \{(\boldsymbol{x}_i, y_i)\}_{i=1}^{n} \tag{8}$$

where $\boldsymbol{x}_i \in \mathbb{R}^d$ are the input features, and $y_i \in \mathbb{R}$ represents the corresponding target value for the i^{th} sample. Suppose there are M distinct base learners $f_m(\boldsymbol{x})$, where $m = 1, 2, \cdots, M$. Each base model produces a prediction for the input x_i, as formulated as:

$$\widehat{y}_i^m = f_m(\boldsymbol{x}_i) \tag{9}$$

where $\widehat{y}_i^m$ represents the predicted output for the i^{th} sample generated by the m^{th} base learner. These individual predictions are then aggregated to form a new feature vector for each sample:

$$\boldsymbol{z}_i = \left[\widehat{y}_i^{(1)}, \widehat{y}_i^{(2)}, \cdots, \widehat{y}_i^{M}\right]^T \tag{10}$$

This transformed vector $\boldsymbol{z}_i \in \mathbb{R}^M$ is used as the input to a meta-learner function $g(\cdot)$, which is trained to generate the final prediction:

$$\widehat{y}_i = g(\boldsymbol{z}_i) \tag{11}$$

In matrix form, the stacking ensemble process over the full dataset can be expressed as:

$$\widehat{y} = g(F(\mathrm{X})) \tag{12}$$

where $F(\mathbf{X}) \in \mathbb{R}^{n \times M}$ is the matrix of base model predictions over the dataset X and $g(\cdot)$ is denotes the meta-model function. Depending on the modeling objective and performance requirements, this function can take the form of a simple regressor, such as LR, or a more sophisticated learner like LSBoost [49].

This approach is particularly suitable when the base learners are diverse in nature, such as combining GPR, SVR, RF, LSBoost, and MLP, as explored in this study. Each of these models contributes unique insights, and their ensemble through stacking leads to more stable and accurate leaching yield predictions. Moreover, stacking is not dependent on any specific type of regression model and does not require strong assumptions about the underlying data. This characteristic allows it to integrate various learning algorithms, making it flexible and easily adaptable to different applications. In the subsequent section, the implementation details of the proposed stacking model architecture, including the design of base and meta-learners, as well as training strategies, are thoroughly discussed.

3. The proposed model for leaching yield prediction

3.1. Stacking model architecture and implementation

To address the complex, nonlinear, and interacting effects observed in leaching processes, a stacking ensemble learning approach was adopted in this study. The overall architecture of the proposed stacking-based model is illustrated in Fig. 3, which is structured into three distinct phases: (1) data processing & partitioning, (2) base model training, and (3) meta learning & final prediction.

Phase 1: Data processing and partitioning

In the first phase, raw experimental data is subjected to preprocessing procedures, including min–max normalization, to ensure all input features are scaled to fall within the [0, 1] range. This normalization prevents any single feature from dominating the learning process due to scale differences. Subsequently, the normalized data are partitioned using k-fold cross-validation with k set to 10 to enhance model generalization and reduce the risk of overfitting. A portion of the data is reserved as the test set, while the remaining folds are used for training and validation, as illustrated in Fig. 3. To support the selection of this configuration, a comparative evaluation of different k values (from 5 to 10) is presented in Table S2 of the Supplementary Material.

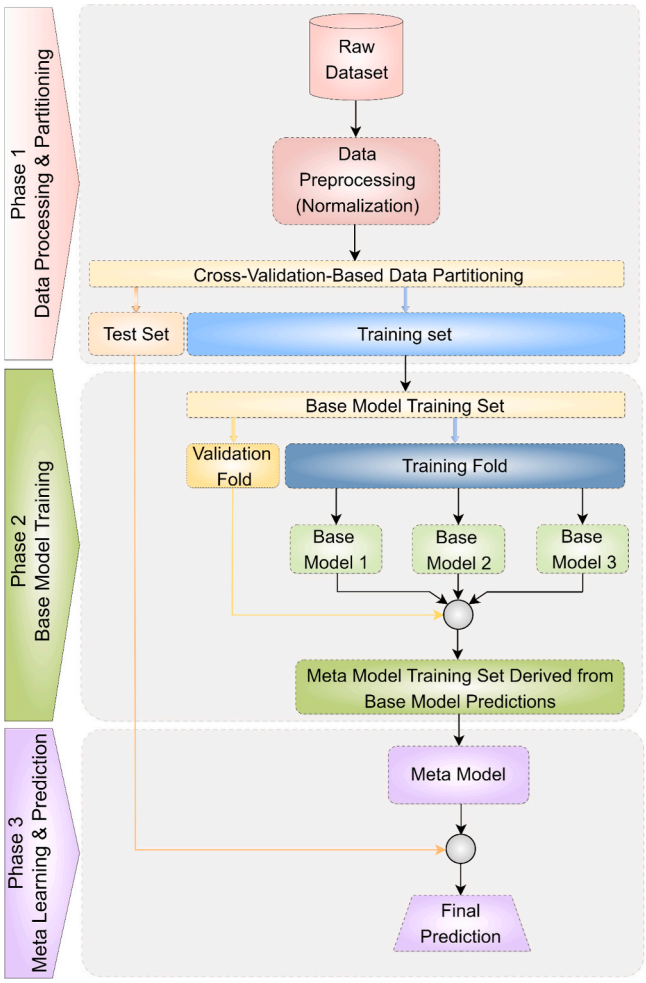

Fig. 3. Block diagram of the proposed stacking-based model for leaching yield prediction.

Phase 2: Base model training

The second phase focuses on training three diverse base models: GPR, LSBoost, and SVR. Each model is trained on the training fold and validated on a separate validation fold. This phase aims to capture different perspectives from the data by training three base models, each selected for its specific strengths:

- GPR was selected due to its probabilistic nature and capacity to model nonlinear relationships while also providing uncertainty estimation, which is critical in complex chemical systems like leaching.
- LSBoost, a gradient boosting method, effectively addresses bias and variance by iteratively improving weak learners, making it robust and highly accurate in handling noise and variability in data.
- SVR was included for its strength in managing high-dimensional spaces and ensuring generalization through margin maximization and kernel-based mapping.

These models individually generate predictions for the validation set, and their outputs collectively form a new feature set called the meta-model training set. Bayesian optimization was used to determine the optimal hyperparameters for each base learner. This technique efficiently explores the hyperparameter space, balancing exploration and exploitation to minimize prediction error. The best hyperparameters determined using Bayesian optimization for each base learner are shown in Table 2. These configurations represent the parameter settings that yielded the best performance according to the evaluation metrics detailed in Section 3.2.

Phase 3: Meta learning and final prediction

In the final phase, the stacked output generated by the base models during Phase 2 is used to train a meta-learner. Specifically, a linear regression (LR) model is used as the meta-model due to its computational simplicity, interpretability, and effectiveness in learning optimal linear combinations of various predictions. The meta-learner takes as input the combined predictions from the base learners (GPR, LSBoost, and SVR) and generates a new feature space representing higher-level patterns of the original data.

By assigning appropriate weights to each base learner's output, the LR meta-model captures the complementary strengths of the base models and compensates for their weaknesses. This layered learning structure enhances the generalization capacity of the overall ensemble by allowing the meta-learner to refine predictions based on patterns that any single base model may not have fully captured.

The stacking process, including base and meta-learning, is integrated within a *k*-fold cross-validation system to provide a fair and unbiased evaluation. In each fold, the meta-model is trained using predictions from the base learners and then tested on a corresponding hold-out set. The final performance is the average of all folds, as seen in Fig. 3. This repeated validation procedure provides a robust estimate of the model's real-world prediction capability by minimizing partition-dependent bias. The final predictions produced by the meta-learner are evaluated using a set of performance metrics to assess the proposed method's accuracy and reliability. These metrics and their corresponding results are detailed in the following subsection.

3.2. Performance metrics for model evaluation

The evaluation of an ML model's predictive performance requires statistical metrics that quantify its accuracy, reliability, and generalization capability [52]. In this study, four regression performance metrics are employed to assess the effectiveness of the proposed stacking model and its base learners: root mean squared error (RMSE), mean absolute error (MAE), mean absolute percentage error (MAPE), and the coefficient of determination (R^2). Their mathematical formulations are outlined below.

The RMSE measures the standard deviation of residuals, providing an indication of how far the predicted values deviate from the actual values [53]. A lower RMSE indicates a better fit of the model:

$$RMSE = \sqrt{\frac{1}{n}\sum_{i=1}^{n}(y_i - \hat{y}_i)^2} \tag{13}$$

y_i represents the actual leaching yield of the i^{th} sample, and $\hat{y}_i$ denotes the predicted value, and n is the total number of samples. Since RMSE penalizes larger errors more significantly due to squaring, it is particularly useful when significant deviations are of concern [53].

The MAE represents the average absolute differences between actual and predicted values, offering an intuitive measure of model accuracy:

$$MAE = \frac{1}{n}\sum_{i=1}^{n}|y_i - \hat{y}_i| \tag{14}$$

Unlike RMSE, MAE treats all deviations equally and does not emphasize larger errors disproportionately, making it a suitable metric when all errors are considered equally important [53].

To assess the relative error in percentage form, the MAPE is employed, which normalizes the absolute prediction errors by the actual values:

$$MAPE = \frac{100}{n}\sum_{i=1}^{n}\left|\frac{y_i - \hat{y}_i}{y_i}\right| \tag{15}$$

where the multiplication of 100 converts the value into a percentage. MAPE is beneficial in cases where relative errors must be analyzed, though it may become unreliable when the actual values are close to zero [52].

Finally, R^2 measures the proportion of variance in the dependent variable that is explained by the model [53,54]. It is given by:

$$R^2 = 1 - \frac{\sum_{i=1}^{n}(y_i - \hat{y}_i)^2}{\sum_{i=1}^{n}(y_i - \bar{y})^2} \tag{16}$$

where $\bar{y}$ represents the mean of the actual values, the R^2 value ranges from 0 to 1, where values closer to 1 indicate a stronger correlation between predicted and actual values, signifying better predictive performance.

These four performance metrics collectively provide a comprehensive evaluation of the predictive capabilities of the models, ensuring that both absolute and relative errors, as well as model explainability, are effectively analyzed. In the subsequent sections, these metrics are employed to compare the individual base learners and the proposed stacking model to determine their effectiveness in leaching yield prediction.

Table 2
Optimized hyperparameter settings for base learners used in the stacking model.

Base learner	Hyperparameter	Optimized value
GPR	Kernel function	matern32
	Kernel scale	0.7613
	Sigma	1.1113
LSBoost	Number of trees	92
	Max num splits	6
	Min leaf size	1
	Learning rate	0.38535
SVR	Kernel function	Gaussian
	Kernel scale	0.52
	Epsilon	0.014579
	Box constraint (C)	132

4. Results and discussion

4.1. Correlation analysis and feature importance for leaching yield prediction

The correlation analysis was conducted to evaluate the relationships between experimental parameters and their influence on leaching yield. To achieve this, the Pearson correlation matrix was used to examine linear relationships between variables in the leaching process. This method quantifies both the strength and direction of relationships, helping to identify the most influential factors [55]. Fig. 4 presents the Pearson correlation matrix for the experimental parameters and their relationship with the leaching yield. In the heatmap, darker shades represent stronger correlations. The analysis identifies stirring speed (0.625) and H_2O_2 concentration (0.621) as the most influential factors. This strong positive correlation suggests that increased agitation enhances mass transfer and may also disrupt the passive layer, while H_2O_2, as an oxidizing agent, facilitates metal dissolution and improves extraction rates. The highest correlation observed was 0.625 (stirring speed), whereas the lowest was −0.189 (between H_2O_2 and acid molarity), reflecting a weak inverse relationship. The S/L ratio (0.139) and temperature (0.184) exhibited weaker positive correlations. While a

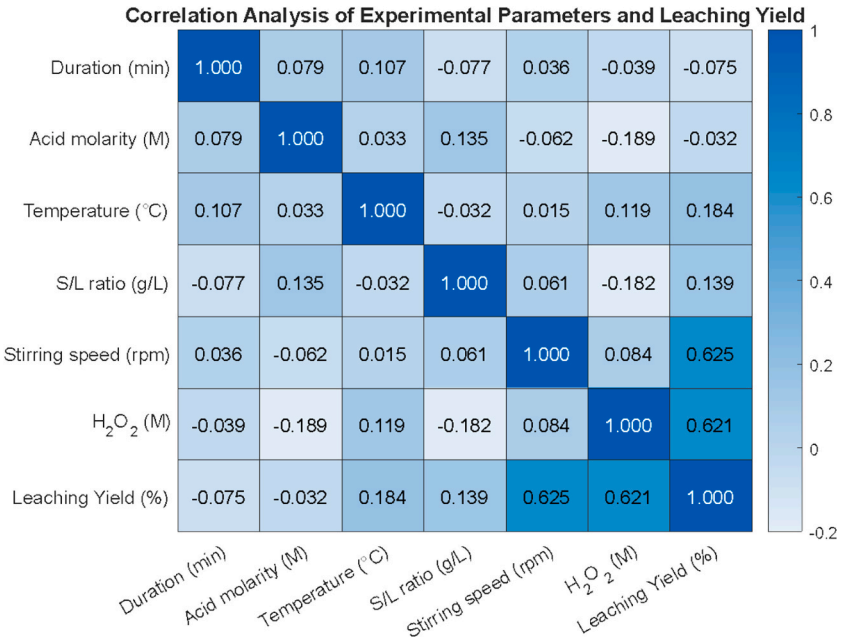

Fig. 4. Correlation analysis of experimental parameters and leaching yield.

higher S/L ratio may slightly improve efficiency, its impact is limited compared to stirring speed and oxidant concentration. Although temperature generally accelerates chemical reactions, its low correlation suggests other factors may play a more dominant role. In contrast, leaching time (−0.075) and acid molarity (−0.032) showed negligible correlations. Prolonged reaction time does not necessarily improve efficiency, possibly due to reagent depletion, while sulfuric acid concentration alone appears to have minimal impact on leaching yield. This limited influence may be attributed to the high SiO_2 content in the waste powder (as confirmed by the XRD analysis in Fig. 2), which can lead to silica gel formation. This gel layer potentially hinders the dissolution of copper into the leaching solution over time. Moreover, as the acid concentration increases, silica gel formation tends to become more pronounced, further intensifying this inhibitory effect [56]. Among all process parameters, stirring speed and H_2O_2 concentration (0.084) exhibited the strongest interrelation, hinting at a possible interaction effect. The S/L ratio and temperature (−0.032) revealed a weak negative correlation, indicating limited influence on S/L distribution. Overall, stirring speed and H_2O_2 concentration emerge as the key determinants of leaching efficiency, while acid molarity and duration appear less significant. Optimizing stirring speed and oxidant concentration can improve leaching performance, while further regression modeling may reveal underlying nonlinear dependencies.

While correlation analysis provides insights into linear relationships between parameters, it does not fully capture the nonlinear interactions within the system [57]. To address this limitation, feature importance analysis was performed using recursive feature elimination (RFE) with GPR to identify the most influential parameters more precisely. As illustrated in Fig. 5, the two most critical experimental variables were determined as stirring speed (rpm) and H_2O_2 concentration (M). These parameters received the highest importance scores, confirming their substantial influence on leaching efficiency. Among them, stirring speed (rpm) emerged as the most influential factor, highlighting the role of mass transfer enhancement in leaching efficiency. Higher agitation rates improve reactant diffusion and facilitate effective contact between the leaching solution and solid particles, thereby accelerating dissolution. This result is consistent with previous studies emphasizing hydrodynamic conditions as a key driver of metal recovery [58,59]. Similarly, H_2O_2 concentration also played a dominant role, functioning as a strong oxidizing agent that promotes metal dissolution through oxidative

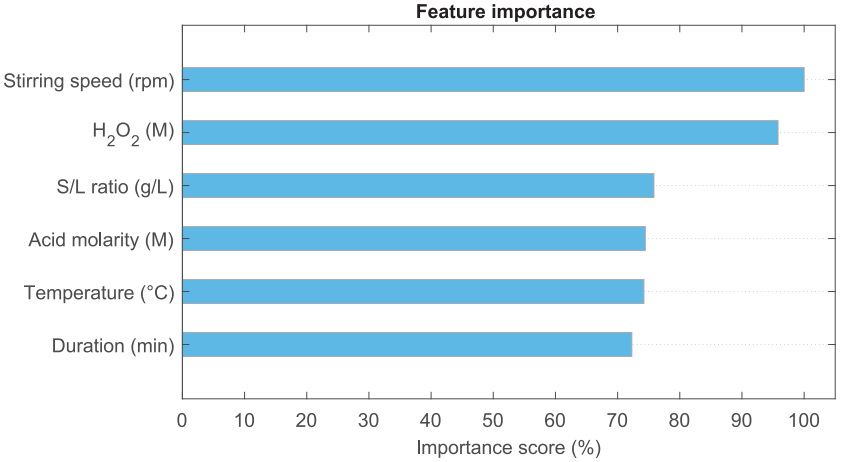

Fig. 5. Importance score of leaching conditions.

reactions. However, excessive H_2O_2 levels may trigger side reactions, making precise dosage control essential to avoid inefficiencies. Although the remaining parameters exhibit some influence on leaching efficiency, their impact is comparatively lower. These secondary factors may contribute under specific conditions or interact with dominant variables, necessitating further investigation to uncover potential nonlinear dependencies. These findings reinforce the necessity of advanced regression modeling to establish a robust predictive framework for process optimization.

In summary, while linear correlation highlights the primary drivers of leaching yield, feature importance analysis through RFE with GPR further substantiates the dominance of stirring speed and oxidant concentration. These findings validate their prioritization in advanced predictive modeling and process optimization.

4.2. Assessment of prediction models for leaching yield

This section compares the performance of five commonly used regression models (GPR, SVR, RF, LSBoost, and MLP) and evaluates them against the proposed stacking ensemble model. The evaluation was conducted using standard statistical metrics, including RMSE, MAE, MAPE, and R^2.

Fig. 6 presents the comparison between actual and predicted leaching yields (left) and the corresponding parity plots (right) for each model. While most models can capture the overall trend, the proposed stacking model exhibits a notably tighter alignment with the experimental values, particularly in regions with higher variability. This is further supported by the zoomed-in views included within each model's visualization, where specific regions of interest are marked with green dashed boxes to examine local prediction behavior more closely. Among all models, the proposed model demonstrates greater consistency and accuracy in capturing these localized variations. Additionally, the parity plots illustrate the strong agreement between predicted and actual values. The proposed model achieves an R^2 of 0.9944, outperforming all individual models.

The performance metrics of all models, including their mean values

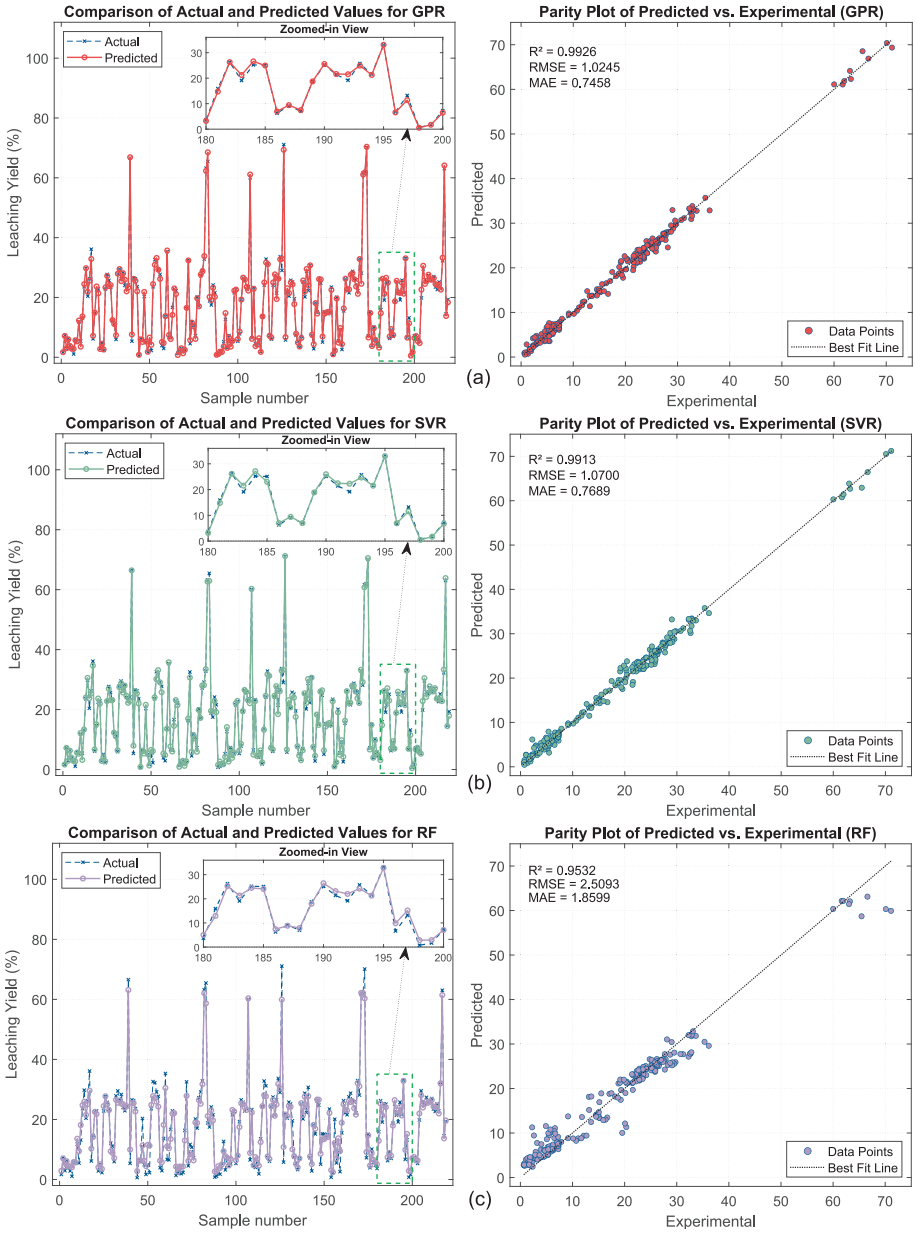

Fig. 6. Comparison of actual and predicted leaching yields (left) and parity plots (right) for different ML models: (a) GPR, (b) SVR, (c) RF, (d) LSBoost, (e) MLP, and (f) the proposed model.

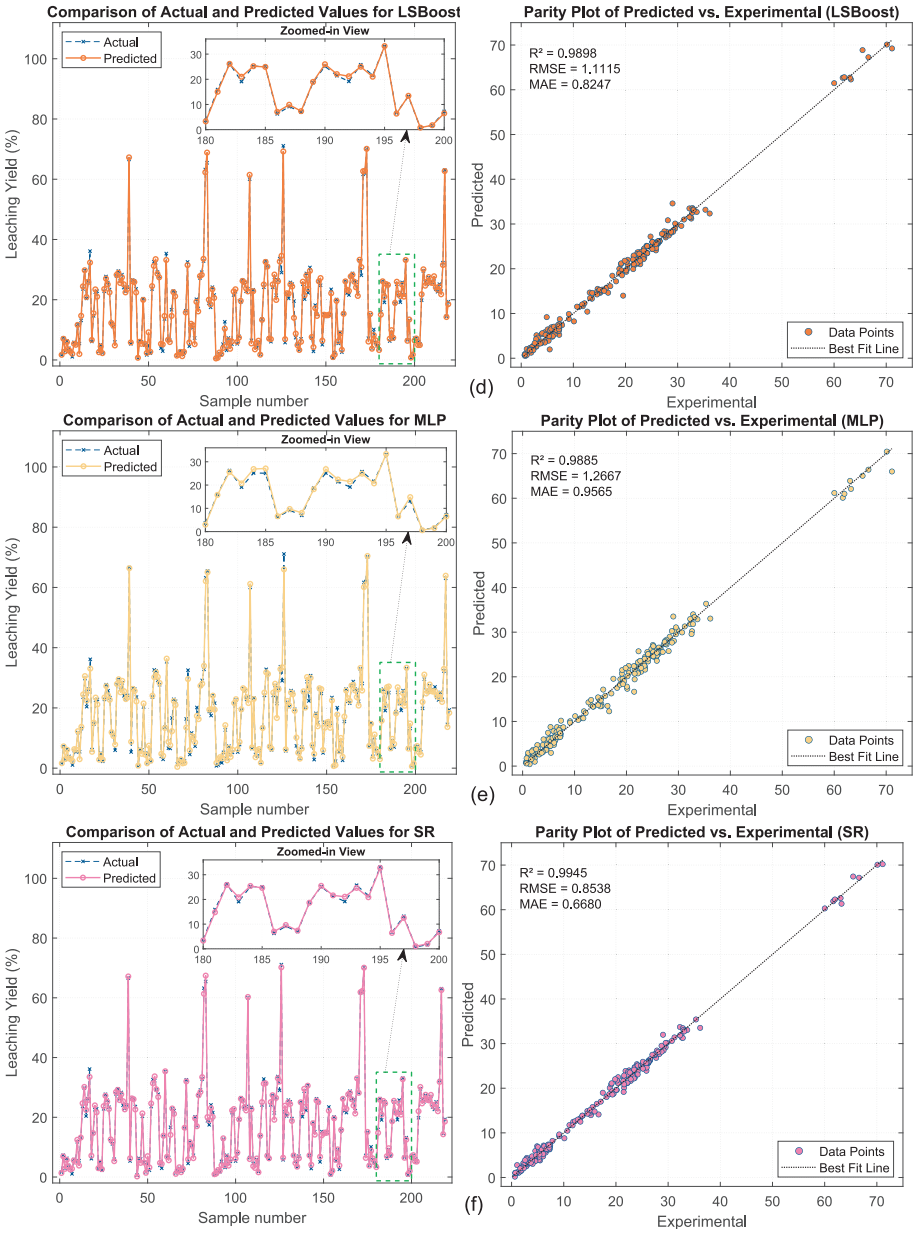

Fig. 6. (*continued*).

and standard deviations over 10-fold cross-validation, as well as the average model training and prediction times for each approach, are presented in Table 3. Among the evaluated methods, the proposed stacking ensemble consistently achieved the best results, recording the lowest RMSE (0.8538 ± 0.193), MAE (0.668 ± 0.141), and MAPE (8.347 % ± 3.91), as well as the highest R^2 value (0.9944 ± 0.0037). These results indicate not only high predictive accuracy but also low prediction variance, reflecting strong generalization capability. GPR and SVR also demonstrated competitive performance with RMSE values of 1.0245 ± 0.125 and 1.0700 ± 0.197, respectively. Although their accuracy metrics are close to that of the proposed model, the slightly higher error margins and larger standard deviations suggest less stable performance under cross-validation. In contrast, the RF model exhibited the poorest performance, with a significantly high RMSE of 2.5093 ± 0.958 and an MAPE of 29.97 % ± 17.48, underscoring its sensitivity to nonlinearities and data heterogeneity in the leaching yield prediction. While LSBoost and MLP showed moderate predictive performance, with MAPE values of 9.01 % ± 3.91 and 11.56 % ± 6.37, respectively, both models were clearly outperformed by the stacking ensemble in terms of both accuracy and stability.

Table 3
Performance metrics and computation time of individual and proposed models.

Prediction model	RMSE (±Std)	MAE (±Std)	MAPE (%) (±Std)	R^2 (±Std)	Computation time (s)
GPR	1.0245 ± 0.125	0.7458 ± 0.109	8.3657 ± 3.659	0.9926 ± 0.0038	0.47
SVR	1.0700 ± 0.197	0.7689 ± 0.139	10.016 ± 5.517	0.9912 ± 0.0057	0.14
RF	2.5093 ± 0.958	1.8599 ± 0.725	29.966 ± 17.48	0.9531 ± 0.0394	0.02
LSBoost	1.1115 ± 0.316	0.8246 ± 0.171	9.0098 ± 3.912	0.9897 ± 0.0096	0.63
MLP	1.2667 ± 0.286	0.9565 ± 0.143	11.564 ± 6.374	0.9885 ± 0.0069	7.25
The proposed method	0.8538 ± 0.193	0.6680 ± 0.141	8.3478 ± 3.914	0.9944 ± 0.0037	1.73

Overall, the proposed model not only outperformed all individual learners in terms of average error but also clearly demonstrated its effectiveness in providing robust regression for complex chemical systems. These findings emphasize the effectiveness of ensemble learning in improving predictive accuracy. By integrating the strengths of diverse base learners, the stacking model successfully reduces generalization error and captures complex interactions within the leaching process more effectively than individual models.

In terms of computational performance, the proposed stacking ensemble model required an average of 1.73 s for training and prediction, which is slightly higher than most individual models. Nevertheless, this increase is justifiable given the substantial improvements in accuracy and stability. Furthermore, unlike real-time applications such as autonomous navigation or robotic control, leaching processes operate on much longer time scales, typically ranging from several minutes to hours, where millisecond-level predictions are not essential. Within this context, prioritizing prediction accuracy and robustness over computational speed makes the modest overhead of the stacking ensemble a reasonable and effective trade-off. Notably, the stacking architecture was intentionally designed using three base learners: GPR, SVR, and LSBoost. These models were selected not only for their complementary predictive strengths but also for their computational efficiency, as reflected in their relatively low computation times (0.47 s for GPR, 0.14 s for SVR, and 0.63 s for LSBoost). This strategic selection ensured that the overall ensemble remains practical and scalable for data-driven modeling tasks. For instance, although the MLP model yielded moderate prediction accuracy, it incurred the highest computation time (7.25 s), indicating inefficiency in resource usage. Conversely, the RF model achieved the shortest computation time (0.02 s) but exhibited the poorest prediction accuracy, rendering it unsuitable for the task. From this perspective, the proposed stacking model offers a favorable trade-off between computational cost and predictive performance, particularly in offline or near-real-time settings where high precision and stability are prioritized.

Residual error distributions of all regression models are illustrated in Fig. 7, offering insights into model bias, prediction dispersion, and robustness. Among the evaluated models, the proposed method demonstrates the most consistent and centered residual behavior, with a near-zero median (0.0047), the narrowest interquartile range (Q1 = –0.449, Q3 = 0.551), and compact whisker boundaries (–2.96 to 2.61). These indicators reflect a balanced prediction pattern with minimal systematic bias and high generalization capability across different data subsets. GPR and SVR models also yield residual distributions closely centered around zero (medians of –0.0059 and –0.0030, respectively), indicating low bias. However, their broader interquartile ranges and larger whisker spans suggest increased variability in prediction accuracy. Notably, SVR exhibits the highest number of outliers (14), implying reduced resilience against extreme deviations. In contrast, the RF model shows significant prediction instability, with a negatively skewed residual median (–0.0850), the widest interquartile range (–1.44 to 1.09), and extreme whisker values extending from –9.01 to 11.19. This pattern reflects a high degree of error dispersion and a tendency toward inconsistent predictions. Similarly, LSBoost and MLP models reveal wider error ranges and moderate bias, though to a lesser extent than RF. Overall, the residual analysis presented in Fig. 7 reinforces the superiority of the stacking ensemble. It effectively reduces prediction errors while maintaining low dispersion and high reliability, making it a robust choice for complex regression tasks such as leaching yield prediction.

4.2.1. *Contribution analysis of base models in the stacking ensemble*

To better understand how the stacking ensemble integrates information from different base models during prediction, a contribution analysis was conducted based on the weight coefficients assigned by the meta-learner. As shown in Fig. 8(a), LSBoost and GPR received the highest average weights, with values of 5.09 and 5.07, respectively. These values indicate that the ensemble structure relied heavily on these two models to generate accurate predictions.

On the other hand, SVR was assigned a comparatively lower average weight of 3.71. Despite this, SVR played a significant role in specific cases. As depicted in Fig. 8(b), the fold-wise RMSE distribution reveals that SVR outperformed the other models in fold 2 and fold 7, where it achieved the lowest RMSE among all base learners. This outcome highlights SVR's ability to contribute valuable predictive insight under certain data conditions.

These findings support the idea that even a model with a relatively smaller average contribution can enhance the performance of the ensemble when it captures distinct patterns within specific data subsets. Therefore, including SVR as a base learner improved the overall diversity and generalization capability of the proposed stacking framework.

4.3. *Effect of the combination of leaching conditions on the leaching yield*

A comprehensive understanding of the individual effects of leaching parameters is essential for optimizing metal dissolution processes. However, in practice, these variables often interact in complex ways, sometimes synergistically enhancing efficiency and producing opposing

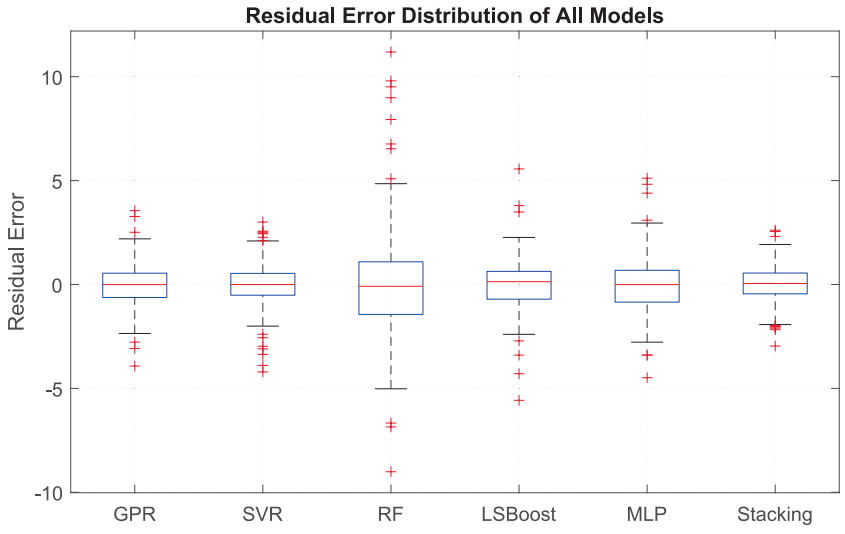

Fig. 7. Boxplot representation of residual errors for all regression models.

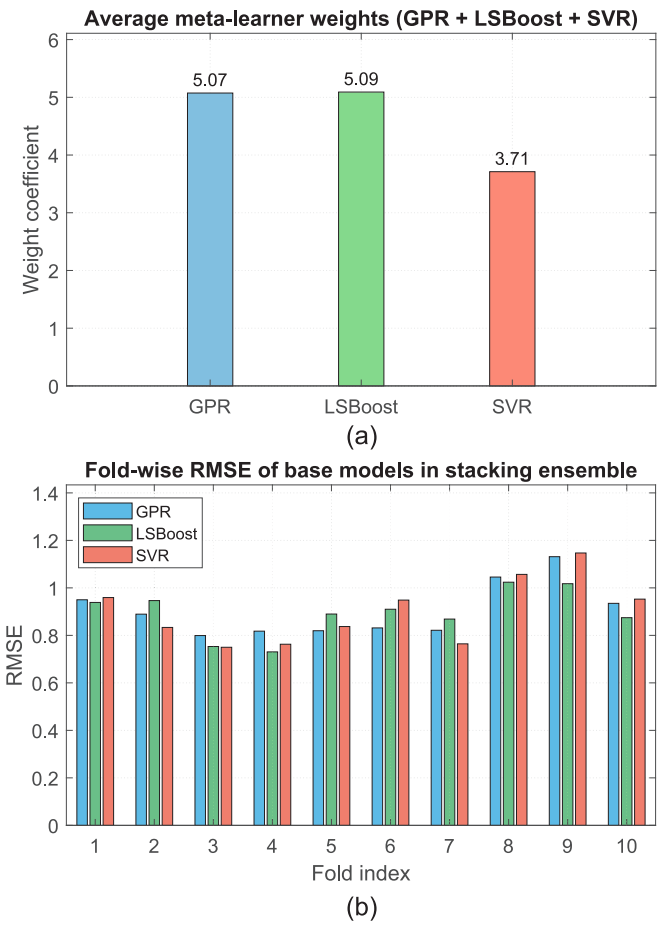

Fig. 8. Contribution and performance distribution of base learners in the stacking ensemble, (a) Average weight coefficients assigned by the *meta*-learner to each base model, (b) Fold-wise RMSE comparison of base models.

effects that hinder overall performance. Since the simultaneous variation of key parameters can lead to nonlinear system responses, it becomes crucial to analyze their combined impact rather than evaluating each factor in isolation. To address this, a detailed analysis was conducted to investigate how selected pairs of experimental variables jointly affect the leaching yield.

As observed in Fig. 9(a), the leaching yield strongly depends on stirring speed and H_2O_2 concentration. At low stirring speeds (<200 rpm) and low H_2O_2 concentrations (<0.5 M), the leaching yield remains below 20 %, indicating insufficient agitation and oxidative potential for effective metal dissolution. However, as the stirring speed increases beyond 400 rpm and the H_2O_2 concentration exceeds 1.0 M, the leaching yield rises sharply, reaching values above 60 %. This suggests that higher agitation enhances mass transfer, while increased oxidant concentration accelerates metal dissolution. Nonetheless, at H_2O_2 concentrations exceeding 1.5 M, a slight decline in leaching yield is observed, likely due to excessive oxidation or the formation of passivating surface layers, which may inhibit further dissolution.

Fig. 9(b) presents the interaction between the S/L ratio and temperature. The results indicate that at low temperatures (20–40 °C) and low S/L ratios (<30 g/L), the leaching yield remains minimal, not exceeding 8 %. However, as the temperature surpasses 60 °C, a significant improvement in leaching efficiency is observed, particularly at an S/L ratio of 80 g/L, where the yield reaches approximately 20 %. At very high S/L ratios (>90 g/L), a slight decline in leaching yield is evident, likely due to diffusion limitations that restrict reagent access to solid particles, leading to incomplete dissolution.

Fig. 9(c) illustrates the combined influence of stirring speed and leaching time on copper leaching yield. At lower stirring speeds (<200 rpm), the leaching yield remains below 20 %, regardless of the leaching duration, indicating that insufficient agitation severely limits mass transfer and hinders copper dissolution. However, when the stirring speed exceeds 400 rpm, a substantial increase in leaching yield is observed, even at short durations (<100 min), with yields approaching 55–60 %. As the leaching time is extended beyond 200 min, the yield continues to increase, reaching up to ~65 % under high stirring conditions. This trend underscores that stirring speed is the dominant factor in enhancing leaching performance, while leaching duration is a secondary variable, further improving yield only when adequate mixing is

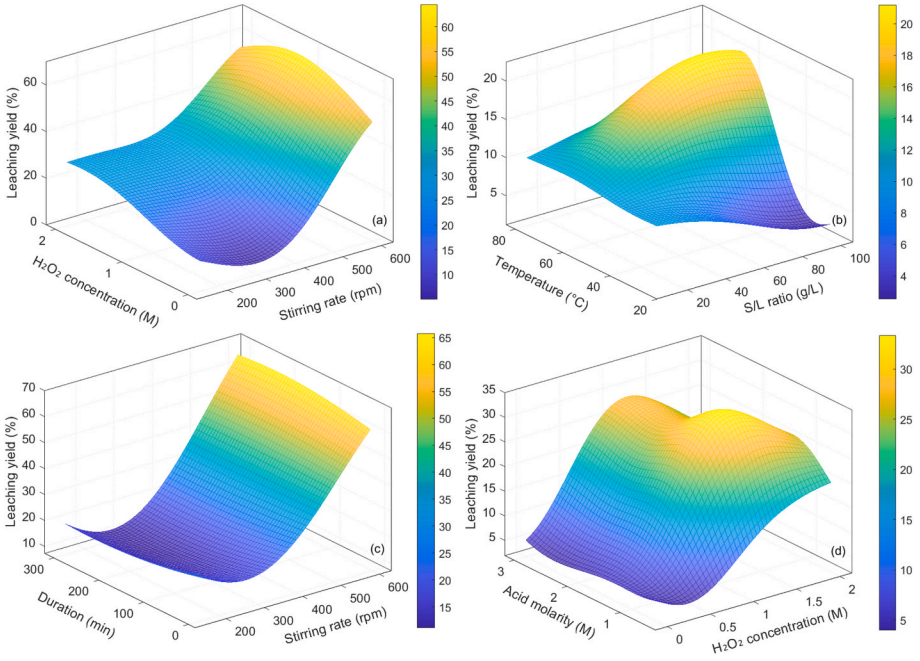

Fig. 9. Influence of combined leaching parameters on the leaching rate, (a) Stirring speed vs·H_2O_2 concentration, (b) S/L ratio vs. temperature, (c) Stirring speed vs. leaching time, (d) H_2O_2 concentration vs. acid molarity.

ensured. Beyond 250 min, the yield follows a flat trend, indicating that the system is approaching a diffusion or reaction equilibrium state. This interpretation is further supported by the feature importance analysis presented in Section 4.2, which identifies stirring speed as the most influential factor, while leaching time exhibits a relatively modest effect on the predictive model.

Fig. 9(d) illustrates the combined influence of acid molarity and H_2O_2 concentration on the leaching yield. As both parameters increase from their lower limits, a steady rise in leaching yield is observed, reaching a maximum of approximately 33 % at around 1.3 M H_2SO_4 and 1.4 M H_2O_2, which is consistent with the findings reported in previous studies [9,31], where sulfuric acid concentrations of 1–2 M and hydrogen peroxide levels of 1–1.5 M were commonly employed to enhance oxidative leaching of copper and zinc from brass slag. Beyond this optimal region, no significant increase is recorded; a slight plateau or mild reduction is observed. This suggests diminishing returns under higher reagent concentrations, although confirming the underlying chemical mechanisms, such as side reactions, oxidant oversaturation, or surface passivation, would require further experimental investigation.

These findings collectively indicate that stirring speed and oxidant concentration are the most influential factors, directly enhancing metal dissolution efficiency. Meanwhile, leaching time and temperature exert a more gradual effect, where their contributions become significant only after surpassing critical thresholds. Due to diffusion constraints, the S/L ratio demonstrates an optimal range beyond which efficiency declines. Furthermore, excess oxidant or acid molarity may induce unwanted side reactions, leading to diminished overall efficiency. Therefore, an optimized balance between these parameters is crucial for maximizing leaching performance, minimizing reagent wastage, and mitigating undesired side effects that may hinder process efficiency.

4.4. Discussion

To provide a broader perspective on the current research, a comparative analysis of recent studies employing ML techniques for metal recovery prediction is presented in Table 4. These studies vary significantly regarding source materials, target metals, and modeling frameworks.

From a source material perspective, most existing studies have predominantly concentrated on primary ores, such as oxide copper ores, Cu Co ores, cerussite, or electronic wastes, including printed circuit boards and spent batteries. These materials are frequently examined in hydrometallurgical research due to their high metal content and significant environmental implications. In contrast, the present study uniquely focuses on brass melting slag, an industrially relevant yet comparatively underexplored secondary waste stream. The reviewed literature does not include studies investigating copper recovery from brass-derived waste using data-driven modeling approaches. This clearly demonstrates the originality of the current study in terms of source material selection.

In terms of the target metal, copper remains the predominant focus in the existing literature, either as the sole element of interest or in conjunction with other metals such as cobalt, zinc, or lead. While the present study is consistent with this general trend, it introduces a significant distinction by investigating copper recovery from an industrial brass slag matrix. This material is characterized by a complex composition that includes metallic and non-metallic phases. The inherent heterogeneity of this matrix poses a greater challenge for modeling efforts and enhances the practical relevance of predictive solutions tailored to such systems.

The modeling approaches adopted in previous studies exhibit considerable diversity, encompassing traditional methods such as ANNs and LR, as well as more sophisticated ensemble techniques including RF, gradient boosting, and XGBoost. Although a limited number of recent studies have investigated hybrid frameworks, such as integrating ANNs with shrinking core models or boosting algorithms, stacked ensemble

Table 4
Overview of ML applications in metal recovery prediction.

Study	Source material	Target metal	Leaching method	Modeling approach	Objective	Input parameters	Output variable	Dataset scope
Ref [23]	Alkaline battery waste	Zn	Alkaline (NaOH) leaching	ANN	Predict Zn recovery	NaOH conc., temp., S/L ratio, time	Zn recovery (%)	Lab-scale (N/R)
Ref [26]	Oxidized/sulfide Cu ore	Cu	Heap leaching (H_2SO_4)	DSS + ML	Decision support for Cu recovery	Oxide %, Sulfide %, Granulometry, Cl^-	Cu recovery (%)	Industrial data (N/R)
Ref [27]	E-waste (PCBs)	Cu	Dynamic acid leaching (H_2SO_4)	ANN, LR	Predict Cu concentration	Stirring, time, acid conc., temp., O_2	Cu (ppm)	96 samples
Ref [28]	Spent Zn–Mn batteries	Zn, Mn	Bioleaching	LR, RF, AdaBoost, GBoost, XGBoost	Maximize Zn and Mn recovery	Substrate conc., pH, temp., pulp density	Zn & Mn (g/L)	29 samples
Ref [29]	Copper oxide ore	Cu	Column leaching	ANN vs. GANN	Optimize Cu recovery	Column height, size, flow rate, Time	Cu recovery (%)	3 columns
Ref [30]	Cerussite concentrate	Pb, Zn	HBF_4 leaching	Gene expression programming (GEP)	Predict Pb and Zn recovery	Acid conc., time, temp., L/S, agitation	Pb & Zn recovery (%)	31 tests
Ref [60]	Low-grade Cu ore	Cu	Cl^- heap leaching	ML + PCA + Naïve Bayes	Predict Cu recovery & heap health	Water, NaCl/$CaCl_2$, Temp., Aeration	Cu recovery (%)	Industrial data (N/R)
Ref [61]	PCBs	Cu	H_2O_2 + Acid leaching	XGBoost, RF, SVM	High recovery prediction	H_2O_2, Acid, Cu %, Time	Cu recovery (%)	1,200 dataset
Ref [62]	Co–Cu ore	Cu, Co	H_2SO_4 leaching	ANN + Shrinking core	Optimize leaching	Acid conc., Temp., Time, Pulp ratio, Stirring	Cu & Co recovery (%)	32 tests
Ref [63]	E-waste (PCBs)	Cu	Hydrometallurgical	ANN + Boosting	Predict Cu recovery	H_2SO_4, H_2O_2, S/L ratio, Time	Cu recovery (%)	Lab data (N/R)
Ref [64]	Cu–Co ores	Cu, Co	Acid leaching	ANN	Optimize Cu/Co leaching	Acid conc., Time, Temp., Pulp density, Reductant	Cu & Co recovery (%)	25 experiments
This study	Brass slag	Cu	Stirred acid leaching	Stacking (GPR + SVR + LSB)	Predict Cu recovery	Time, Temp., H_2O_2, Acid, S/L, Stirring	Cu recovery (%)	219 Lab-experiments

learning remains largely unexplored in this domain. The present study addresses this gap by implementing a stacking ensemble model that combines GPR, SVR, and LSBoost. By harnessing the complementary strengths of these individual learners, the proposed approach enhances both generalization capability and predictive robustness. This improvement is reflected in the model's superior performance across multiple statistical evaluation metrics.

In terms of dataset characteristics, most of the referenced studies are based on limited sample sizes, typically involving a small number of laboratory-scale experiments. While some datasets consist of as few as 25 to 96 samples, studies utilizing industrial data often do not specify the number of observations. In this context, the present study distinguishes itself by employing a dataset composed of 219 laboratory-based experiments, which is comparatively larger and more diverse. This enhanced dataset supports the development of more robust and generalizable predictive models, thereby increasing the practical relevance and reliability of the proposed approach.

The proposed method addresses a significant gap in the literature by presenting a distinctive combination of source material, modeling strategy, and dataset scale. Although brass slag has been previously studied in metallurgical research, its application in data-driven copper recovery prediction remains unexplored. This is the first study to employ ML techniques, specifically a stacked ensemble learning framework, to predict copper yield from brass melting slag. This contribution extends the scope of predictive modeling within hydrometallurgy and introduces a scalable and reliable decision-support tool for valorizing industrial by-products in alignment with circular economy principles.

5. Conclusions

This study presents a robust stacking ensemble learning framework for predicting copper leaching yield from brass melting slags under varying hydrometallurgical process conditions. The proposed model effectively captures the complex, nonlinear interactions among key leaching parameters by integrating experimental data with advanced ML techniques. The hybrid architecture, which combines GPR, LSBoost, and SVR base learners with a linear regression meta-model, was systematically validated using 10-fold cross-validation and comprehensive residual error analyses. The results indicate that the stacking ensemble approach outperforms all individual models' predictive accuracy and generalization ability, offering a scalable and interpretable solution for optimizing copper recovery from metallurgical waste.

The significant findings of this research can be summarized as follows:

1. The proposed stacking model achieved the highest predictive performance among all tested models, with an R^2 of 0.9944 ± 0.0037, RMSE of 0.8538 ± 0.193, MAE of 0.668 ± 0.141, and MAPE of 8.347 % ± 3.91 across 10-fold cross-validation.
2. Stirring speed (0.625) and H_2O_2 concentration (0.621) were identified as the most influential parameters by Pearson correlation analysis.
3. The residual error distribution of the stacking model exhibited minimal bias, a narrow interquartile range (Q1 = –0.449, Q3 = 0.551), and compact whiskers (–2.96 to 2.61), indicating high robustness and prediction stability across folds.
4. RF showed the poorest predictive capability, with an RMSE of 2.5093 ± 0.958 and a highly dispersed residual distribution, underscoring its sensitivity to data heterogeneity and noise.
5. Combined parameter analysis revealed that high stirring speed (>400 rpm), moderate-to-high H_2O_2 concentrations (1.0–1.5 M), and extended leaching times (>200 min) collectively enhance copper recovery, with yield values exceeding 60–65 % under optimal combinations.
6. The stacking model eliminated the need for additional long-term experimental trials by efficiently leveraging pre-existing experimental data, providing a cost-effective and scalable computational framework for process design and parameter optimization.

This research presents a practical and accurate data-driven framework for predicting copper recovery from brass waste. The stacking ensemble architecture achieves high predictive performance while offering clear interpretability of parameter interactions, supporting data-informed decision-making in hydrometallurgical processes. Future studies may extend this model toward multi-objective optimization, incorporate economic and environmental considerations, and adapt the approach for other types of industrial waste. In addition, adopting more advanced modeling strategies such as transformer-based deep learning architectures, ARIMA, or unsupervised clustering techniques (e.g., k-means) could be explored, particularly for larger or more complex datasets. These models may be especially valuable in hybrid ensemble frameworks where their strengths can complement conventional learners for enhanced generalization and feature interaction modeling.

CRediT authorship contribution statement

Sercan Basit: Writing – original draft, Resources, Methodology, Investigation, Formal analysis, Data curation, Conceptualization. **Murat Uyar:** Writing – review & editing, Visualization, Supervision, Software, Methodology, Formal analysis, Conceptualization.

Declaration of competing interest

The authors declare that they have no known competing financial interests or personal relationships that could have appeared to influence the work reported in this paper.

Acknowledgment

This work was partially supported by the Scientific and Technological Research Council of Turkey (TÜBİTAK) under project number 113M241. The authors gratefully acknowledge Dr. Muhlis Nezihi Sarıdede and Dr. Ayfer Kılıçarslan for their valuable support during the experimental design phase. The authors would also like to thank Özer Metal A.Ş. (Çerkezköy, Istanbul, Turkey) for providing the brass waste samples used in this study.

Appendix A. Supplementary data

Supplementary data to this article can be found online at https://doi.org/10.1016/j.seppur.2025.134691.

Data availability

Data will be made available on request.

References

[1] D. Raabe, The materials science behind sustainable metals and alloys, Chem. Rev. 123 (5) (2023) 2436–2608.
[2] T.E. Graedel, E.M. Harper, N.T. Nassar, P. Nuss, B.K. Reck, Criticality of metals and metalloids, Proc. Natl. Acad. Sci. 112 (14) (2015) 4257–4262.
[3] Weick, V. (2016). Green Economy and sustainable development. In *Waste Management and the Green Economy* (pp. 121-150). Edward Elgar Publishing.
[4] F.J. Afshar, G.R. Khayati, The application of superhydrophobic coatings to brass alloy substrates: a review, J. Alloy. Compd. 960 (2023) 170634.
[5] E. Dauvergne, C. Mullié, Brass alloys: copper-bottomed solutions against hospital-acquired infections? Antibiotics 10 (3) (2021) 286.
[6] B. Hutchinson, O. Rod, Brass alloys, Mater. Sci. Technol. 32 (17) (2016) 1743.
[7] https://www.businessresearchinsights.com/market-reports/brass-market-117883.
[8] J.M.A. Martins, A.S. Guimaraes, A.J.B. Dutra, M.B. Mansur, Hydrometallurgical separation of zinc and copper from waste brass ashes using solvent extraction with D2EHPA, J. Mater. Res. Technol. 9 (2) (2020) 2319–2330.
[9] I.M. Ahmed, A.A. Nayl, J.A. Daoud, Leaching and recovery of zinc and copper from brass slag by sulfuric acid, J. Saudi Chem. Soc. 20 (2016) S280–S285.

[10] M.K. Sinha, S.K. Sahu, S. Pramanik, L.B. Prasad, B.D. Pandey, Recovery of high-value copper and zinc oxide powder from waste brass pickle liquor by solvent extraction, Hydrometallurgy 165 (2016) 182–190.
[11] A. Fattah-alhosseini, M. Molaei, M. Kaseem, A review on the plasma electrolytic oxidation (PEO) process applied to copper and brass, Surf. Interfaces (2024) 104179.
[12] F. Maleki, S. Ghasemi, A. Heidarpour, Recycling of brass melting slag through the high-temperature oxidation-leaching process, Sustain. Environ. Res. 32 (1) (2022) 24.
[13] Z. Xia, X. Zhang, X. Huang, S. Yang, Y. Chen, L. Ye, Hydrometallurgical stepwise recovery of copper and zinc from smelting slag of waste brass in ammonium chloride solution, Hydrometallurgy 197 (2020) 105475.
[14] Y. Huang, D. Wang, H. Liu, G. Fan, W. Peng, Y. Cao, Selective complexation leaching of copper from copper smelting slag with the alkaline glycine solution: an effective recovery method of copper from secondary resource, Sep. Purif. Technol. 326 (2023) 124619.
[15] Y. Desai, R.R. Srivastava, V.K. Srivastava, G. Kaushik, V.K. Singh, Hydrometallurgical recovery of critical metals from an incinerated fly ash of municipal solid waste from western India, Geosyst. Eng. 26 (5) (2023) 208–217.
[16] A. Sobouti, F.S. Hoseinian, B. Rezai, S. Jalili, The lead recovery prediction from lead concentrate by an artificial neural network and particle swarm optimization, Geosyst. Eng. 22 (6) (2019) 319–327.
[17] Z. Zhang, X. Zhang, D. Zhang, X. Zhang, F. Qiu, W. Li, C. Tang, Application of machine learning in a mineral leaching process— taking pyrolusite leaching as an example, ACS Omega 7 (51) (2022) 48130–48138.
[18] J.A. Barragan, J.R. Aleman Castro, A.A. Peregrina-Lucano, M. Sánchez-Amaya, E. P. Rivero, E.R. Larios-Durán, Leaching of metals from e-waste: from its thermodynamic analysis and design to its implementation and optimization, ACS Omega 6 (18) (2021) 12063–12071.
[19] J. Hao, X. Wang, Y. Wang, Y. Wu, F. Guo, Optimizing the leaching parameters and studying the kinetics of copper recovery from waste printed circuit boards, ACS Omega 7 (4) (2022) 3689–3699.
[20] D. Packwood, L.T.H. Nguyen, P. Cesana, G. Zhang, A. Staykov, Y. Fukumoto, D. H. Nguyen, Machine learning in materials chemistry: an invitation, Mach. Learn. Appl. 8 (2022) 100265.
[21] M. Kamkar, K.C. Leonard, I. Ferrer, S.C.J. Loo, E.J. Biddinger, D. Brady, J. F. Serrano, Artificial Intelligence (AI) for sustainable resource management and chemical processes, ACS Sustain. Resour. Manage. 1 (2) (2024) 178–180.
[22] P. Mokarian, I. Bakhshayeshi, F. Taghikhah, Y. Boroumand, E. Erfani, A. Razmjou, The advanced design of bioleaching process for metal recovery: a machine learning approach, Sep. Purif. Technol. 291 (2022) 120919.
[23] N. Muñoz García, J.L. Valverde, B. Delgado Cano, M. Heitz, A. Avalos Ramirez, Selective recovery of zinc from alkaline batteries via a basic leaching process and the use of a machine learning-based digital twin for predictive purposes, Energies 17 (24) (2024) 6292.
[24] C. Leiva, V. Flores, F. Salgado, D. Poblete, C. Acuña, Applying soft computing for copper recovery in leaching process, Sci. Program. 2017 (1) (2017) 6459582.
[25] V. Flores, C. Leiva, A comparative study on supervised machine learning algorithms for copper recovery quality prediction in a leaching process, Sensors 21 (6) (2021) 2119.
[26] M. Saldaña, P. Neira, V. Flores, P. Robles, C. Moraga, A decision support system for changes in operation modes of the copper heap leaching process, Metals 11 (7) (2021) 1025.
[27] M. Ordaz-Oliver, E. Jiménez-Muñoz, E. Gutiérrez-Moreno, C.E. Borja-Soto, P. Ordaz, J.F. Montiel-Hernández, Application of artificial neural networks for recovery of Cu from electronic waste by dynamic acid leaching: a sustainable approach, Waste Biomass Valoriz. 15 (12) (2024) 7057–7076.
[28] J. Priyadarshini, M. Elangovan, M. Mahdal, M. Jayasudha, Machine-learning-assisted prediction of maximum metal recovery from spent zinc–manganese batteries, Processes 10 (5) (2022) 1034.
[29] F.S. Hoseinian, A. Abdollahzade, S.S. Mohamadi, M. Hashemzadeh, Recovery prediction of copper oxide ore column leaching by hybrid neural genetic algorithm, Trans. Nonferrous Met. Soc. Chin. 27 (3) (2017) 686–693.
[30] A. Sobouti, B. Rezai, M.T. Rayati, F.S. Hoseinian, The recovery prediction of Zn and Pb from cerussite leaching using the fluoroboric acid by gene expression programming, Sep. Sci. Technol. 56 (1) (2021) 194–202.
[31] A. Kilicarslan, M.N. Saridede, Treatment of industrial brass wastes for the recovery of copper and zinc, Sep. Sci. Technol. 50 (2) (2015) 286–291.
[32] S. Kappal, Data normalization using median median absolute deviation MMAD based Z-score for robust predictions vs. min–max normalization, London J. Res. Sci.: Nat. Formal 19 (4) (2019) 39–44.
[33] T.T. Wong, P.Y. Yeh, Reliable accuracy estimates from k-fold cross validation, IEEE Trans. Knowl. Data Eng. 32 (8) (2019) 1586–1594.
[34] E. Schulz, M. Speekenbrink, A. Krause, A tutorial on Gaussian process regression: modelling, exploring, and exploiting functions, J. Math. Psychol. 85 (2018) 1–16.
[35] S.S. Ghosh, U. Khati, S. Kumar, A. Bhattacharya, M. Lavalle, Gaussian process regression-based forest above ground biomass retrieval from simulated L-band NISAR data, Int. J. Appl. Earth Obs. Geoinf. 118 (2023) 103252.
[36] J. Wu, X.Y. Chen, H. Zhang, L.D. Xiong, H. Lei, S.H. Deng, Hyperparameter optimization for machine learning models based on Bayesian optimization, J. Electron. Sci. Technol. 17 (1) (2019) 26–40.
[37] A.H. Victoria, G. Maragatham, Automatic tuning of hyperparameters using Bayesian optimization, Evol. Syst. 12 (1) (2021) 217–223.
[38] E. Li, F. Yang, M. Ren, X. Zhang, J. Zhou, M. Khandelwal, Prediction of blasting mean fragment size using support vector regression combined with five optimization algorithms, J. Rock Mech. Geotech. Eng. 13 (6) (2021) 1380–1397.
[39] W. Zhang, D. Liu, K. Cao, Prediction of concrete compressive strength using support vector machine regression and non-destructive testing, Case Stud. Constr. Mater. 21 (2024) e03416.
[40] Z. El Mrabet, N. Sugunaraj, P. Ranganathan, S. Abhyankar, Random forest regressor-based approach for detecting fault location and duration in power systems, Sensors 22 (2) (2022) 458.
[41] M.H. Lipu, M.A. Hannan, A. Hussain, S. Ansari, S.A. Rahman, M.H. Saad, K. M. Muttaqi, Real-time state of charge estimation of lithium-ion batteries using optimized random forest regression algorithm, IEEE Trans. Intell. Veh. 8 (1) (2022) 639–648.
[42] H. Tahraoui, A. Amrane, A.E. Belhadj, J. Zhang, Modeling the organic matter of water using the decision tree coupled with bootstrap aggregated and least-squares boosting, Environ. Technol. Innov. 27 (2022) 102419.
[43] D.J. Godwin, E.G. Varuvel, M.L.J. Martin, Prediction of combustion, performance, and emission parameters of ethanol powered spark ignition engine using ensemble least squares boosting machine learning algorithms, J. Clean. Prod. 421 (2023) 138401.
[44] A. Mosavi, S. Samadianfard, S. Darbandi, N. Nabipour, S.N. Qasem, E. Salwana, S. S. Band, Predicting soil electrical conductivity using multi-layer perceptron integrated with grey wolf optimizer, J. Geochem. Explor. 220 (2021) 106639.
[45] A. Masaea, M. Kubokale, A.K. Kumar, R.R. Kumar, M.H. Assaf, S. Kumar, Ground simulation and pattern recognition for arbitrary distance optical transmission of a free-space laser communication system, IEEE Access 12 (2024) 118695–118705.
[46] M.J. Van der Laan, E.C. Polley, A.E. Hubbard, Super learner, Stat. Appl. Genet. Mol. Biol. 6 (1) (2007).
[47] A.I. Naimi, L.B. Balzer, Stacked generalization: an introduction to super learning, Eur. J. Epidemiol. 33 (2018) 459–464.
[48] D. Kansara, R. Singh, D. Sanghvi, P. Kanani, Improving accuracy of real estate valuation using stacked regression, Int. J. Eng. Dev. Res 6 (3) (2018) 571–577.
[49] M.G. Meharie, W.J. Mengesha, Z.A. Gariy, R.N. Mutuku, Application of stacking ensemble machine learning algorithm in predicting the cost of highway construction projects, Eng. Constr. Archit. Manag. 29 (7) (2022) 2836–2853.
[50] M.H.D.M. Ribeiro, L. dos Santos Coelho, Ensemble approach based on bagging, boosting and stacking for short-term prediction in agribusiness time series, Appl. Soft Comput. 86 (2020) 105837.
[51] Y. Cao, G. Liu, J. Sun, D.P. Bavirisetti, G. Xiao, PSO-Stacking improved ensemble model for campus building energy consumption forecasting based on priority feature selection, J. Build. Eng. 72 (2023) 106589.
[52] Y. Tan, W. Xu, K. Yang, S. Pasha, H. Wang, M. Wang, Q. Xiao, Predicting cobalt ion concentration in hydrometallurgy zinc process using data decomposition and machine learning, Sci. Total Environ. 962 (2025) 178420.
[53] D. Chicco, M.J. Warrens, G. Jurman, The coefficient of determination R-squared is more informative than SMAPE, MAE, MAPE, MSE and RMSE in regression analysis evaluation, PeerJ Comput. Sci. 7 (2021) e623.
[54] D. Zhang, A coefficient of determination for generalized linear models, Am. Stat. 71 (4) (2017) 310–316.
[55] S. Kumar, P. Rani, An AI-based liver disease prediction model based on pearson correlation feature selection method, Biomed. Pharmacol. J. 17 (4) (2024) 2187–2202.
[56] A.N. Banza, E. Gock, K. Kongolo, Base metals recovery from copper smelter slag by oxidising leaching and solvent extraction, Hydrometallurgy 67 (1–3) (2002) 63–69.
[57] N. Sharma, Y.A. Liu, A hybrid science-guided machine learning approach for modeling chemical processes: a review, AIChE J. 68 (5) (2022) e17609.
[58] I. Nozari, A. Azizi, Experimental and kinetic modeling investigation of copper dissolution process from an Iranian mixed oxide/sulfide copper ore, J. Sustain. Metall. 6 (2020) 437–450.
[59] E.S.A. Haggag, M.S. Khalafalla, A.M. Masoud, Leaching kinetics of uranium, rare earth elements and copper using tartaric acid from El Allouga ore material, Southwestern Sinai, Egypt, Int. J. Environ. Analyt. Chem. 103 (20) (2023) 8561–8576.
[60] H. Kaschel, J.A. Pérez, A.Z. Cipriano, M. Millán. (2023, December). A Machine Learning Approach to Recovery Optimization for Copper Chloride Leaching Process. In *2023 IEEE CHILEAN Conference on Electrical, Electronics Engineering, Information and Communication Technologies (CHILECON)* (pp. 1-6). IEEE.
[61] S. Daware, S. Chandel, B. Rai, A machine learning framework for urban mining: a case study on recovery of copper from printed circuit boards, Miner. Eng. 180 (2022) 107479.
[62] M. Mathaba, J. Banza, Application of machine learning approach (artificial neural network) and shrinking core model in cobalt (II) and copper (II) leaching process, J. Environ. Sci. Health A 59 (1) (2024) 25–32.
[63] S.K. Srivastava, R. Shrivastava, Modeling for copper recovery from e-waste by using machine learning technique: an approach for the circular economy, Curr. Analyt. Chem. (2025), https://doi.org/10.2174/0115734110343714241130170537.
[64] K.K. Brest, K.J.J. Monga, M.M. Henock, (2021, January). Implementation of Artificial Neural network into the copper and cobalt leaching process. In *2021 Southern African Universities Power Engineering Conference/Robotics and Mechatronics/Pattern Recognition Association of South Africa (SAUPEC/RobMech/PRASA)* (pp. 1-5). IEEE.